

# Comparing Bayesian Models for Organ Contouring in Head and Neck Radiotherapy

Prerak P Mody<sup>a</sup>, Nicolas Chaves-de-Plaza<sup>b</sup>, Klaus Hildebrandt<sup>b</sup>, René van Egmond<sup>c</sup>, Huib de Ridder<sup>c</sup>, and Marius Staring<sup>a</sup>

<sup>a</sup>Department of Radiology, Leiden University Medical Center, Leiden, The Netherlands

<sup>b</sup>Computer Graphics and Visualization Lab, TU Delft, Delft, The Netherlands

<sup>c</sup>Industrial Design Engineering, TU Delft, Delft, The Netherlands

## ABSTRACT

Deep learning models for organ contouring in radiotherapy are poised for clinical usage, but currently, there exist few tools for automated quality assessment (QA) of the predicted contours. Using Bayesian models and their associated uncertainty, one can potentially automate the process of detecting inaccurate predictions. We investigate two Bayesian models for auto-contouring, DropOut and FlipOut, using a quantitative measure – expected calibration error (ECE) and a qualitative measure – region-based accuracy-vs-uncertainty (R-AvU) graphs. It is well understood that a model should have low ECE to be considered trustworthy. However, in a QA context, a model should also have high uncertainty in inaccurate regions and low uncertainty in accurate regions. Such behaviour could direct visual attention of expert users to potentially inaccurate regions, leading to a speed-up in the QA process. Using R-AvU graphs, we qualitatively compare the behaviour of different models in accurate and inaccurate regions. Experiments are conducted on the MICCAI2015 Head and Neck Segmentation Challenge and on the DeepMindTCIA CT dataset using three models: DropOut-DICE, Dropout-CE (Cross Entropy) and FlipOut-CE. Quantitative results show that DropOut-DICE has the highest ECE, while Dropout-CE and FlipOut-CE have the lowest ECE. To better understand the difference between DropOut-CE and FlipOut-CE, we use the R-AvU graph which shows that FlipOut-CE has better uncertainty coverage in inaccurate regions than DropOut-CE. Such a combination of quantitative and qualitative metrics explores a new approach that helps to select which model can be deployed as a QA tool in clinical settings.

**Keywords:** Radiotherapy, Segmentation, Uncertainty, Bayesian Deep Learning, DropOut, FlipOut, Entropy

## 1. INTRODUCTION

The contouring task in radiotherapy is time-consuming and is subject to inter- and intra-annotator disagreement. As deep learning models have made great progress in this field,<sup>1</sup> they are widely being considered as an automated technique to speed up and standardize the contouring process. However, to deploy such models in a clinical setting, a manual quality assessment (QA) of predicted contours needs to be performed before they can be used for radiation planning, which again introduces a delay. This work investigates the potential usage of uncertainty heatmaps produced by Bayesian deep learning models to help speed up the manual QA process, by directing human attention to inaccurate regions.

In a classification setting, a predictive model is calibrated when its output probabilities (i.e. maximum softmax value) corresponds to the likelihood of being accurate\*. It has been shown that well-calibrated models also produce uncertainty measures that correspond to inaccurate regions.<sup>2</sup> To further investigate this in a QA context, for the purpose of choosing a model for clinical deployment, two Bayesian models were analysed - DropOut<sup>2</sup> and FlipOut.<sup>3</sup> We use a combination of a quantitative metric - expected calibration error (ECE)<sup>4</sup> and a qualitative metric - region-based accuracy-vs-uncertainty (R-AvU) graphs. Since some models may provide us with similar ECE values, we use the R-AvU graphs that plot the uncertainty probabilities in accurate and inaccurate regions to understand the difference in the behavior of such models. We chose entropy as the uncertainty metric, since it allows us to capture both model (epistemic) and data (aleatoric) uncertainty.

Further author information: (Send correspondence to P.P.M.)

P.P.M.: E-mail: P.P.Mody@lumc.nl

\*In a calibrated model, voxels predicted to belong to a class with probability  $p$ , should have an accuracy equal to  $p$ .

## 2. METHOD

### 2.1 Data

CT scans along with annotations for 9 organs at risk (OAR) in the head-and-neck area were used from the MICCAI2015-Head and Neck Segmentation Challenge dataset.<sup>5</sup> This dataset provided 33 training and 10 test samples. Models trained on this dataset were also evaluated on a separate dataset titled DeepMindTCIA,<sup>6</sup> containing 15 patients. Each CT volume is resampled to a resolution of (0.8, 0.8, 2.4) mm and cropped with a bounding box of dimensions (240,240,80) around the brainstem. The Hounsfield units were trimmed from -125 to +225 to better capture contrast for soft tissues. The models consumed random 3D patches of size (140,140,40) that were augmented with 3D translations, 3D rotations and 3D deformations.

### 2.2 Neural Architecture

The base convolutional neural network (CNN) of our Bayesian models is inspired by FocusNet,<sup>1</sup> a deterministic model, with the exception that we do not use their supplementary network for smaller organs. Our models add Bayesian layers in the DenseASPP module of FocusNet which forms the middle layers of FocusNet. We use either DropOut<sup>2</sup> ( $p = 0.25$ ) or FlipOut<sup>3</sup> layers, which perform activation space and weight space perturbations during each forward pass, respectively. These layers perform variational inference on the model weights (i.e. posterior estimation) by either applying a Bernoulli distribution on neural activations (DropOut) or assuming the space of weights to be a fully factorizable Gaussian (FlipOut). The DropOut model contains  $\sim 500k$  parameters, while the FlipOut model contains twice those parameters due to the Gaussian assumption. The models produce activation maps for each OAR and a softmax function followed by the argmax operator is used to assign it an OAR class.

The models are trained using either soft-DICE or cross-entropy (CE) loss. The CE loss penalizes both the false negative voxels i.e.  $L = \mathbb{1}_{(y=1)} \cdot \log(p)$  in each OAR’s activation map, and false positive voxels i.e.  $L = \mathbb{1}_{(1-y)=1} \cdot \log(1 - p)$ . Here,  $y = \{0, 1\}$  is the ground truth class of a voxel and  $p$  is the softmax probability in context of a single OAR’s activation map. To train the FlipOut model, one minimizes the CE loss as well as the KL-Divergence term between the Gaussian prior and posterior.<sup>3</sup>

### 2.3 Inference and Evaluation

During inference, Monte Carlo sampling (M=30) approximates the model posterior which is used to produce OAR activation maps. These are then averaged to produce OAR class predictions as described above. ECE is calculated for each OAR as specified in<sup>4</sup> with 10 equally spaced bins between 0 and 1. Using the activation maps, we compute entropy maps and average them across Monte Carlo samples. They are used to compute the R-AvU graph which consists of a line plot for the probability of uncertainty in inaccurate ( $p(u|i)$ ) regions as well as the probability of uncertainty in accurate ( $p(u|a, \sim a)$ ) regions. We define accurate regions as those containing true positive (TP) voxels. We include the  $\sim a$  term to denote *almost* TP voxels, as due to inter- and intra-observer variation, it is common to disregard false positive (FP) and false negative (FN) voxels close to the ground truth. This is done by an erosion-dilation process on the inaccurate regions using a (3,3,1) filter. The remaining FP and FN voxels are included in the inaccurate regions.

## 3. EXPERIMENTS AND RESULTS

We train and evaluate 3 Bayesian models c.f. DropOut-DICE, DropOut-CE and FlipOut-CE along with their deterministic variants. Figure 1 shows for both datasets that Dropout-DICE and DropOut-CE always have lower ECE than their deterministic counterparts Dropout-Dice-Det and DropOut-CE-Det. DropOut-CE on average has a lower ECE than DropOut-DICE, while FlipOut-Det and FlipOut-CE have similar ECE. The same holds for DropOut-CE and FlipOut-CE. Note that all models have equivalent performance in terms of standard medical segmentation metrics, i.e DICE ( $\sim 0.77 - 0.78$ ) and Hausdorff Distance 95% ( $\sim 5\text{mm} - 7\text{mm}$ ).

Figure 2 represents  $p(u|i)$  as solid line plots and  $p(u|a, \sim a)$  as dotted line plots. A model for efficient QA would have high  $p(u|i)$  and low  $p(u|a, \sim a)$ . The  $p(u|i)$  of the FlipOut-CE model is higher than that of the DropOut-CE model for the entire range of thresholds, though the inverse holds true for  $p(u|a, \sim a)$ . The DropOut-DICE model maintains a fixed value for  $p(u|i)$  and  $p(u|a, \sim a)$  up till thresholds less than  $10^{-1}$ . It

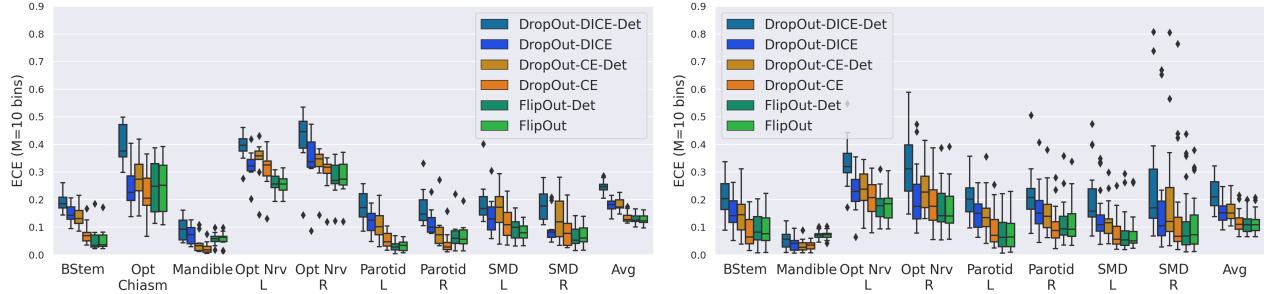


Figure 1. Boxplot depicting the Expected Calibration Error (ECE) with  $M=10$  bins for the MICCAI2015 test dataset (left) and the DeepMindTCIA dataset (right). The x-axis shows the different organs and the average.

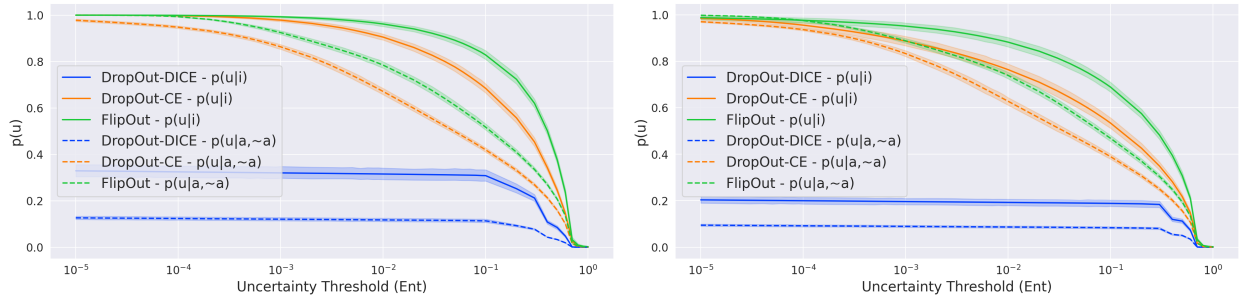


Figure 2. Line plots showing the uncertainty behaviour of different models in inaccurate ( $p(u|i)$ ) and accurate ( $p(u|a, \sim a)$ ) regions for the MICCAI2015 test set (left) and the DeepMindTCIA dataset (right).

always has values lower than DropOut-CE and FlipOut-CE for both  $p(u|i)$  and  $p(u|a, \sim a)$ . Similar trends are noticed for the DeepMindTCIA dataset, though the probability values are slightly reduced.

The first two rows in Figure 3 shows results from the MICCAI2015 test dataset with the first row representing a false positive prediction for the top slice of the brainstem and the second row representing a true positive prediction for the parotid gland. The third row represents a true positive prediction for the mandible from the DeepMindTCIA dataset.

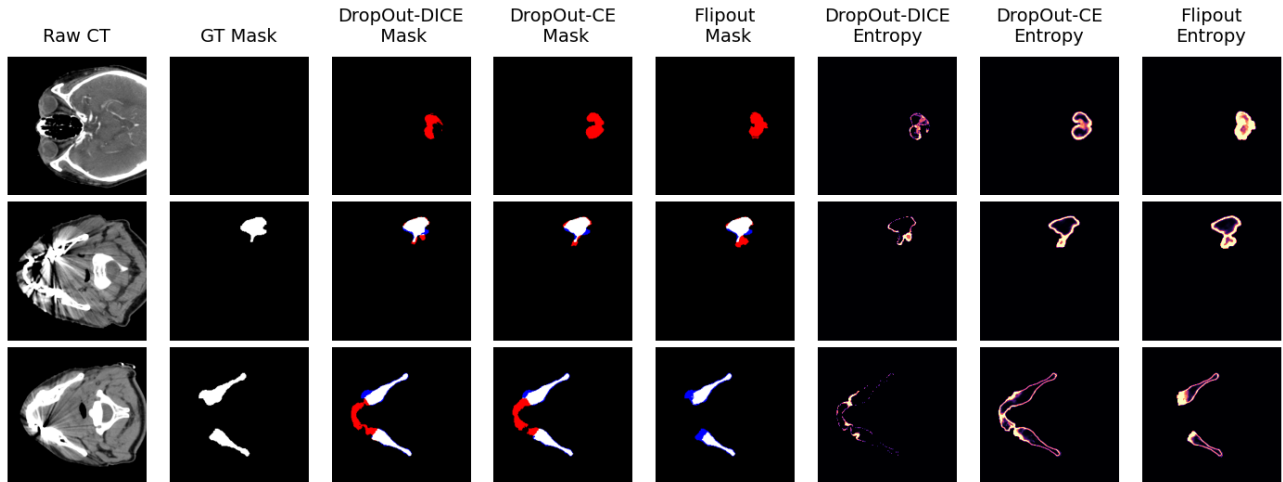


Figure 3. The first two columns depict the raw and ground truth data from the datasets, while the remaining columns show model predictions and their associated uncertainty heatmaps. In the predicted masks, white voxels are true positives, red voxels are false positives while blue voxels are false negatives.

## 4. DISCUSSION AND CONCLUSION

This work exploited an existing deterministic model (i.e. FocusNet<sup>1</sup>) and investigated the calibration and uncertainty behavior of its Bayesian versions for the purpose of efficient QA in a clinical radiotherapy setting. All Bayesian models, when averaged across organs at risk, performed equally well in terms of volumetric and surface distance measures, allowing for a valid comparison across any choice of metrics. While previous work usually shows lower results for models trained with cross entropy when compared to DICE,<sup>2</sup> our use of a modified loss, overcomes that limitation.

The boxplot in Figure 1 shows that performing Bayesian inference in neural networks always reduces or maintains calibration error (ECE). Also, CE as a loss function leads to reduced ECE compared to DICE, as also found by others.<sup>2</sup> It is important for a predictive model to be calibrated as it produces softmax probability estimates that reflects its true underlying interpretation of a test sample, leading to more informative uncertainty heatmaps. Given that DropOut-CE and FlipOut-CE have similar ECE values, we refer to the R-AvU graphs and notice that FlipOut-CE has better uncertainty coverage in inaccurate regions. This is reflected in Figure 2 where both its  $p(u|i)$  and  $p(u|a, \sim a)$  curves are higher than that of DropOut-CE. This means that FlipOut-CE misses less inaccurate regions than DropOut-CE, but also directs visual attention to areas that are accurate, more so than DropOut-CE, potentially slowing down QA. Dropout-DICE, which has the highest ECE, has uncertainty curves that do not sufficiently cover incorrect regions, thus reducing its potential as a contour QA candidate. Focusing on the bright areas in Figure 3, we can see that the first and third row show that FlipOut-CE provides a better coverage of erroneous regions, while in the second row all heatmaps correctly indicate a contouring error.

To conclude, we show that considering false positive and false negative regions in the cross entropy loss provides improved model performance with the additional benefit of improved calibration. We also explored how the combined use of a quantitative and qualitative measure supports the analysis and selection of Bayesian models. It was observed, that on average, FlipOut-CE has more uncertainty coverage of both inaccurate and accurate regions than the DropOut models, possibly due to weight space perturbations. Future work may consider applying this approach in a contour propagation scenario for adaptive radiotherapy.

## ACKNOWLEDGMENTS

The research for this work was funded by the HollandPTC-Varian Consortium (grant id 2019022).

## REFERENCES

- [1] Gao, Y., Huang, R., Chen, M., Wang, Z., Deng, J., Chen, Y., Yang, Y., Zhang, J., Tao, C., and Li, H., “FocusNet: Imbalanced large and small organ segmentation with an end-to-end deep neural network for head and neck CT images,” in [*International Conference on Medical Image Computing and Computer-Assisted Intervention*], 829–838, Springer (2019).
- [2] Sander, J., de Vos, B. D., Wolterink, J. M., and Išgum, I., “Towards increased trustworthiness of deep learning segmentation methods on cardiac MRI,” in [*Medical Imaging 2019: Image Processing*], **10949**, 1094919, International Society for Optics and Photonics (2019).
- [3] LaBonte, T., Martinez, C., and Roberts, S. A., “We know where we don’t know: 3D Bayesian CNNs for credible geometric uncertainty,” *arXiv preprint arXiv:1910.10793* (2019).
- [4] Guo, C., Pleiss, G., Sun, Y., and Weinberger, K. Q., “On calibration of modern neural networks,” in [*International Conference on Machine Learning*], 1321–1330, PMLR (2017).
- [5] Raudaschl, P. F., Zaffino, P., Sharp, G. C., Spadea, M. F., Chen, A., Dawant, B. M., Albrecht, T., Gass, T., Langguth, C., Lüthi, M., et al., “Evaluation of segmentation methods on head and neck CT: Auto-segmentation challenge 2015,” *Medical physics* **44**(5), 2020–2036 (2017).
- [6] Nikolov, S., Blackwell, S., Zverovitch, A., Mendes, R., Livne, M., De Fauw, J., Patel, Y., Meyer, C., Askham, H., Romera-Paredes, B., Kelly, C., Karthikesalingam, A., Chu, C., Carnell, D., Boon, C., D’Souza, D., Moinuddin, S. A., Garie, B., McQuinlan, Y., Ireland, S., Hampton, K., Fuller, K., Montgomery, H., Rees, G., Suleyman, M., Back, T., Hughes, C. O., Ledsam, J. R., and Ronneberger, O., “Clinically applicable segmentation of head and neck anatomy for radiotherapy: Deep learning algorithm development and validation study,” *J Med Internet Res* **23**, e26151 (Jul 2021).